Segmentation of Natural Scene Images using Grating Cell Texture Operator and K-means Clustering Algorithm

Jajnyadatta Samantaray*, Nrusingha Prasad Rath**, Neeharika Naik***
*, **, *** Department of Electronics, Veer Surendra Sai University of Technology Burla, Odisha
*jajnya@yahoo.co.in, ** n_p_rath@hotmail.com, ***neeharikabputece@gmail.com

Abstract— Texture is an attribute which is so easy to be visually recognized but hard to be mathematically characterized. In this paper, a grating cell texture operator has been proposed that responds vigorously to texture present in the form of grating of bars of appropriate orientation, position and periodicity. The scene images similarly represent a consistent texture in natural objects (e.g. mountain, grass, trees etc.) which respond to the grating cell. In the images, the texture of different objects of scene varies from one another. Thus, the grating cell responds differently to different objects of a scene image for a given set of parameters which is the criteria for segmentation. The textural properties of an image are stored in a feature matrix which is given to k-means clustering algorithm for segmentation purpose.

Keywords— k-means clustering; scene-segmentation; grating cell.

Introduction

The task of partitioning a natural image into regions with homogeneous texture, commonly referred to as image segmentation, is widely accepted as a crucial function for high-level image understanding, significantly reducing the complexity of content analysis of images. Dominant criteria for measuring segmentation performance are based on qualitative and quantitative comparisons with human segmentation results. The rapid accumulation of large collections of digital images has created the need for efficient and intelligent schemes for image retrieval. Since manual annotation of large image databases is both expensive and time consuming, it is desirable to base such schemes directly on image content.

Indeed, the field of Content-Based Image Retrieval (CBIR) has made significant advances in recent years. One of the most important and challenging components of many CBIR systems is scene segmentation. The objects of scene images like mountain, tree, grass etc. show the characteristics of texture like variations in roughness, smoothness, regularity etc. These extracted features constitute the feature vector which is analyzed further to segment scene images. Each object reflects a specific textural property which differentiates it from other object of the scene and it is the basis of segmentation in scene images.

Peter Kruizinga and Nikolay Petkov [1] have proposed a texture operator known as grating cell which consists of simple cells. Such cells respond vigorously to a grating of bars of appropriate orientation, position and periodicity. We have used this operator in our paper for texture analysis in scene images and finally k-means clustering algorithm has been used for the segmentation of scene images.

Junqing Chen et al [2] have presented an approach for image segmentation that is based on low-level features for color and texture. The proposed approach combines knowledge of human perception with an understanding of signal characteristics in order to segment natural scenes into perceptually/semantically uniform regions.

Longsheng WEI et al [3] have proposed an active contour texture image segmentation method based on anisotropic diffusion. Their method is based on an observation that texture in a relatively local region is separable, despite of the inseparability of the texture in the whole image caused by the texture complicacy.

Xiuwen Liu et al [4] have presented a new segmentation method for images consisting of texture, as well as non texture regions using local spectral histograms. By decomposing the algorithm into three stages, they have derived probability models and couple feature extraction with segmentation through iterative updating.

S. Kothainachiar et al [5] have extracted low level features such as color and texture using adaptive clustering algorithm and texture complex wavelet decomposition respectively. Then, the smooth region of image is segmented using morphological watershed, and non smooth region is segmented using multi-grid region growing.

Tao et al [6] have incorporated the advantages of the mean shift (MS) segmentation and the normalized cut (N-cut) partitioning methods, in their proposed method which requires low computational complexity and is therefore very feasible for real-time image segmentation processing.

Mishra et.al [7] have used the fixation point of human eye as an identification marker on the object and proposed a method to segment the object of interest by finding the optimal closed contour around the fixation point in the polar space, avoiding the

perennial problem of scale in the Cartesian space.

Bosch et.al.[10] have presented a scene description and segmentation system capable of recognizing natural objects (e.g. sky, trees, grass) under different outdoor conditions .They have proposed a hybrid and probabilistic classifier of image regions as a first step in solving the problem of scene context generation. They have focused their work in the problem of image regions labeling to classify every pixel of a given image into one of several predefined classes. The result is both a segmentation of the image and recognition of each segment as a given object class or as an unknown segmented object.

Xiaoru Wang et al.[11] have segmented scene images using a semantics based segmentation algorithm. First the image is transformed to HSV color space because it matches better to human perception. Then region growth algorithm is used for initial segmentation. The color feature of two pixels is defined as their Euclidean distance. For each pixel the Euclidean distance of 8 connected neighbor pixels are calculated. If the distance is less than a threshold then they will be merged and color mean, area, center of the new region is calculated. After that regions are merged based on their similarity value. They have experimented their work using Microsoft research Cambridge object recognition image dataset and mean error rate is 10.9%.

Chang et al[12] have segmented outdoor scene images based on background recognition and Perceptual organization model. Initially they have applied segment and merge technique to generate a set of improved super pixels. Most of the super pixels approximately correspond to object parts in the scene. They built a graph G=(V,E) to represent these super pixels. Where V is the set of pixels and E is the set of edges. Then they have applied background classifier to divide V into two parts. They have separated background objects which are unstructured objects(uniform appearance) from the rest of the image which contain structured objects by textonization process.. After the background is separated, using POM the remaining patches of the foreground can be grouped. For this they have picked one part and then keep growing the region by trying to group its neighbors with region. The process stops when non of the regions neighbors can be grouped with the region. They have tested their work using Berkeley dataset and achieved a success rate of 53%.

The rest of the paper is organized as follows: grating cell texture operator and its application in segmentation of synthetic texture are discussed in section-II. An algorithm is proposed in section-III that computes the feature vector of scene images which can be used for the segmentation using k-means clustering. Some experimental results are provided in section-IV. In section-V, the paper is concluded with some critical analysis.

Grating Cell Construction and Segmentation of Synthetic Texture

Von der Heydt et al. (1991) [9] have proposed the model of a certain type of orientation selective cell found in areas V1 and V2 of the visual cortex of monkeys known as grating cell which responds vigorously to a grating of bars of appropriate orientation, position and periodicity but very weakly or not at all to single bars. The activities of displaced semi-linear units of another type of orientation selective cell known as simple cell are combined by an AND-type nonlinearity to produce grating cell activity, that is the response of a grating cell is computed using as input, the response of simple cells with symmetric receptive field profiles and opposite polarity. Hence, for computation of response of grating cell, response of simple cells has to be discussed as a precursor.

Simple Cell

We use the family of two-dimensional (2D) Gabor functions to model the spatial summation properties of simple cells

$$g_{\xi,\eta,\theta,\varphi}(x,y) = \exp\left(-\frac{x'^2+\gamma^2 y'^2}{2\sigma^2}\right)\cos\left(2\pi\frac{x'}{\lambda} + \varphi\right)$$

$$x' = (x-\xi)\cos\theta - (y-\eta)\sin\theta\,,\ y' = (x-\xi)\sin\theta - (y-\eta)\cos\theta \qquad (1)$$

Where the arguments x and y specify the position of a light impulse in the visual field and ξ, η, σ, λ, θ and γ are parameters as follows: (ξ, η) has the same domain Ω as pair (x, y) specifies the center of a receptive field in image coordinates. The standard deviation σ of the Gaussian factor determines the linear size of the receptive field. The ellipticity of the receptive field ellipse is determined by parameter γ and is called spatial aspect ratio. Its range has been found to be $0.23<\gamma<0.92$.The value $\gamma=0.5$ is used for simulations here. The parameter λ is the wavelength of the cosine factor $\cos\left(2\pi\left(\frac{x'}{\lambda}\right) + \varphi\right)$ and its reciprocal $1/\lambda$ is the spatial frequency of the receptive field function. The ratio σ/λ determines the spatial frequency bandwidth of the filter. The spatial frequency bandwidth (in octave) from frequency f1 to f2 is given by $\log_2(\frac{f2}{f1})$. The half response spatial frequency bandwidth b is a function of σ/λ and is given by

$$b = \log_2 \frac{\left(\frac{\sigma}{\lambda}\right) + \frac{1}{\pi}\sqrt{\frac{\ln 2}{2}}}{\left(\frac{\sigma}{\lambda}\right) - \frac{1}{\pi}\sqrt{\frac{\ln 2}{2}}} \qquad \text{Alternatively} \quad \frac{\sigma}{\lambda} = \frac{1}{\pi}\sqrt{\frac{\ln 2}{2}}\,\frac{2^b + 1}{2^b - 1} \tag{2}$$

$\sigma/\lambda = 0.56$ is used in the present simulations.

The parameter $\theta[0,\pi)$ specifies the orientation of the normal and is represented by the axis x' given in equation (1). The parameter φ is the phase offset in the argument of the cosine factor $\cos(2\pi\left(\frac{x'}{\lambda}\right) + \varphi)$ which determines the symmetry of the Gabor function given in equation (1). For φ=0 and π, the function is even or symmetric with respect to the center (ξ, η) of the receptive field, for φ=-π/2 and π/2, the function is antisymmetric or odd and all other cases are antisymmetric mixture of these two. The values of φ used in the simulation are φ=0 for symmetric receptive fields to which we refer as ''center on'', φ=π for symmetric receptive fields to which we refer to as ''center-off'', and φ=-π/2 and φ= π/2 for antisymmetric receptive fields with opposite polarities. Using the above parameterization, the response $s_{\xi,\eta,\lambda,\theta,\varphi}$ of a simple cell modeled by a receptive field function $g_{\xi,\eta,\lambda,\theta,\varphi}(x,y)$ is computed as follows:

1) First an integral, $r_{\xi,\eta,\lambda,\theta,\varphi} = X(\iint f(x,y) g_{\xi,\eta,\lambda,\theta,\varphi}(x,y)\,dxdy)$ (3)

is evaluated where f(x, y) is the input image. X (z) =0 for z<0, X (z) =z for z>=0.2

2) To normalize the simple cell response with respect to the local average luminance of the input image, $r_{\xi,\eta,\lambda,\theta,\varphi}$ is divided by the average gray level $a_{\xi,\eta,\lambda}$ within the receptive field which is computed using the Gaussian factor of the function $g_{\xi,\eta,\lambda,\theta,\varphi}$

$$a_{\xi,\eta,\lambda} = \iint f(x,y)\exp\left(-\frac{(x-\xi)^2 + \gamma^2(y-\eta)^2}{2\sigma^2}\right)dxdy \tag{4}$$

The ratio $r_{\xi,\eta,\lambda,\theta,\varphi}/a_{\xi,\eta,\lambda}$ is proportional to the local contrast within the receptive field of a simple cell.

3) In order to obtain a contrast response function, we use the hyperbolic ratio function to calculate the simple cell response $s_{\xi,\eta,\lambda,\theta,\varphi}$ as follows:

$$s_{\xi,\eta,\lambda,\theta,\varphi} = \begin{cases} 0, & a < 0 \\ X\left(\dfrac{\frac{r_{\xi,\eta,\lambda,\theta,\varphi}}{a_{\xi,\eta,\lambda}} R}{\frac{r_{\xi,\eta,\lambda,\theta,\varphi}}{a_{\xi,\eta,\lambda}} + C}\right), & otherwise \end{cases} \tag{5}$$

Where R and C are the maximum response level and the semi saturation constant respectively.

Grating Cell

The model of grating cells consists of two stages. In the first stage, the responses of grating subunits are computed using as input the responses of center-on and center-off simple cells with symmetrical receptive fields. The model of a grating subunit is conceived in such a way that the unit is activated by a set of three bars with appropriate periodicity, orientation and position. In the, second stage, summation is done on the responses of grating subunits of a given preferred orientation and periodicity within a certain area to compute the response of a grating cell. A quantity $q_{\xi,\eta,\theta,\lambda}$ called the activity of a grating subunit with position (ξ,η), preferred orientation θ and preferred grating periodicity λ is computed as follows:

$$q_{\xi,\eta,\theta,\lambda} = \begin{cases} 1, & if\ \forall n,\ \ M_{\xi,\eta,\theta,\lambda,n} \geq \rho M_{\xi,\eta,\theta,\lambda} \\ 0, & \text{if}\ \exists n,\ \ M_{\xi,\eta,\theta,\lambda,n} < \rho M_{\xi,\eta,\theta,\lambda} \end{cases} \tag{6}$$

Where n ϵ {-3….2}and ρ is a threshold parameter and the auxiliary quantities $M_{\xi,\eta,\theta,\lambda,n}$ and $M_{\xi,\eta,\theta,\lambda}$ are computed as follows:

$$M_{\xi,\eta,\theta,\lambda,n} = \max\{s_{\xi',\eta',\theta,\lambda,\varphi_n} | \xi',\eta':\ n\tfrac{\lambda}{2}\cos\theta \leq (\xi'-\xi) < (n+1)\tfrac{\lambda}{2}\cos\theta,\ \text{and}\ n\tfrac{\lambda}{2}\sin\theta \leq (\eta'-\eta) < (n+1)\tfrac{\lambda}{2}\sin\theta,$$

$$\varphi_n = \begin{cases} 0, & n = -3,-1,1 \\ \pi, & n = -2,0,2 \end{cases} \tag{7}$$

$$M_{\xi,\eta,\theta,\lambda} = \max\{M_{\xi,\eta,\theta,\lambda,n} | n = -3 \ldots .2\} \tag{8}$$

The quantities $M_{\xi,\eta,\theta,\lambda,n}$, n=-3…2,are related to the activities of simple cells with symmetric receptive fields along a line segment of length 3λ passing through point (ξ,η) in orientation θ. This segment is divided in intervals of length λ/2 and the maximum activity of one sort of simple cells, center-on or center-off, is determined in each interval. For instance, $M_{\xi,\eta,\theta,\lambda,-3}$, is the maximum activity of center-on simple cells in the corresponding interval of length λ/2 ; $M_{\xi,\eta,\theta,\lambda,-2}$ is the maximum activity of center-off simple cells in the adjacent interval, etc. Center-on and center-off simple cell activities are alternately used in consecutive intervals.

$M_{\xi,\eta,\theta,\lambda}$ is the maximum among the above interval. It states that, the concerned grating cell subunit will be activated if center-on and center-off cells of the same preferred orientation θ and spatial frequency 1/λ are alternately activated in intervals of length λ/2 along a line segment of length 3λ centered on point (ξ, η) and passing in direction θ. For instance, the condition will be fulfilled for three parallel bars with spacing λ and orientation θ of the normal. In contrast, the condition is not fulfilled by the simple cell activity pattern caused by a single or two bars, only.

In the next, second stage of the model, the response $\omega_{\xi,\eta,\theta,\lambda}$ of a grating cell whose receptive field is centered on point (ξ,η) and which has a preferred orientation θ($\theta\epsilon[0,\pi)$) of the normal to the grating and periodicity λ is computed by weighted summation of the responses of the grating subunits. The model is made symmetrical for opposite directions by taking the sum of grating subunits with orientations θ and θ+π.

$$\omega_{\xi,\eta,\theta,\lambda} = \int \exp\left(-\frac{(\xi-\xi')^2+(\eta-\eta')^2}{2(\beta\sigma)^2}\right)(q_{\xi',\eta',\theta,\lambda} + q_{\xi',\eta',\theta+\pi,\lambda})d\xi' d\eta' \quad (9)$$

The weighted summation is done in order to model the spatial summation properties of grating cells with respect to the number of bars and their length as well as their unmodulated responses with respect to the exact position (phase) of a grating. The parameter β is regarding the size of the area over which effective summation takes place. A value of β=5 results in a good approximation of the spatial summation properties of grating cells.

Grating Cell Features

The texture features proposed here, are based on the grating cell operator (6)–(9). A set of grating cell operators with different preferred orientations θ and preferred periodicities λ is applied to an image, yielding a n-D feature vector in each image point (depending upon the number of filters used). In order to understand the behavior of grating cell response, an image of a bottle (having definite shape) and a textured cloth is considered as shown in fig.1 A set of grating cell operators with eight different preferred orientations θ (θ=22.5˚, 45˚, 67.5˚, 90˚,112.5˚, 135˚, 157.5˚,180˚) and three different preferred wavelengths λ (λ=5.47, λ=8.20, λ=10.93) have been applied on the bottle image, yielding a 24-D feature vector in each image point. Then pixel wise maximum superposition of the 24 filters has been done to obtain the feature matrix.

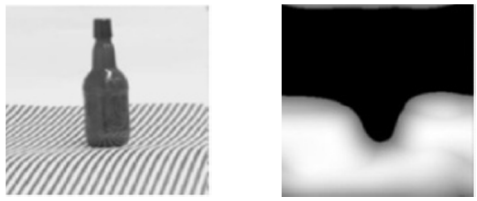

(a) (b)

Fig.1 (a) bottle image (b) grating cell response

From the result, it shows that grating cell texture operator responds to the texture part and doesn't respond at all to the shape of bottle i.e the non-textured part of image.

K-means Clustering Algorithm

The k-means clustering algorithm is used for segmentation. It is based on the following cluster criterion.

$$\vec{x} \in A \text{ if } \forall(B: B \neq A: d(\vec{x},\overrightarrow{\mu_A}) < d(\vec{x},\overrightarrow{\mu_B}) \quad (10)$$

Where A and B are clusters. μ_A and μ_B are the respective mean feature vectors,where each element of the feature vector is a specific pixel value of the output figure of a grating filter. So,the feature vector is n-dimensional where n is the number of grating filters used for computation of feature matrix. and d(x,y) is the distance between two feature vectors x and y. In our experiments we use Euclidean distance. The K-mean clustering procedure is as follows:

- Initially, K cluster mean vectors are chosen randomly.
- Next, all feature vectors are assigned to one of the K clusters using the above criterion.
- Each cluster mean is updated by computing it as the mean of all feature vectors that were assigned to it.
- Steps 2 and 3 are repeated until a certain convergence criterion is fulfilled.

Algorithm for computation of feature matrix and segmentation of scene images

- An input image of size 256x256 is taken.
- Considering mask of size 16 (for highway, forest, mountain, coast) and mask of size 8 (for open country) wavelength (λ=8.2) and orientation (θ=22.5˚, 45˚, 67.5˚, 90˚, 112.5˚, 135˚, 157.5˚, 180˚), the response of the simple cell is computed on the image.
- To process the border pixels, image is padded with same size as mask size.
- By taking as input, the response of center on (φ=0) and center-off ($\varphi=\pi$) simple cells with symmetric receptive fields, the response of grating subunit is computed by using (6).
- Then the responses of grating subunits of orientation and periodicity (as taken above) within an area(β=6) are added together to compute the response of a grating cell using (9).
- For scene images, 8 grating cells having parameters (λ=8.2,θ=22.5˚), (λ=8.2,θ=45˚), (λ=8.2,θ=67.5˚), (λ=8.2, θ=90˚), (λ=8.2,θ=112.5˚), (λ=8.2,θ=135˚), (λ=8.2,θ=157.5˚), (λ=8.2,θ=180˚) is used for the computation of response for a single image and final response can be achieved by the maximum pixel superposition of all the filters' output.
- The matrix so obtained is the feature matrix which contains the textural properties of input image.
- The feature matrix is provided as input to the k-means clustering algorithm to obtain the segmented image.
- Clustering is directly performed on the resultant feature matrix instead of the outputs of all the filters used in the computation of feature matrix.

Experimental results

We have experimented on 100 scene images obtained from [8] considering 20 images from each category. The scenes consist of objects like mountain, water, sky, grass, tree etc. An image of size 256x256 is taken. The simple cell response is computed on the image. In our experiment, wavelength (λ=8.2), orientation (θ=22.5˚,45˚,67.5˚,90˚,112.5˚,135˚,157.5˚,180˚) and mask size 16 have been taken for (coast, mountain, forest, highway) and mask size 8 has been taken (for opencountry). The response of simple cell is computed by performing the convolution of the mask and the input image. Then the maximum response of the simple cells (6 in number) **M** in the particular position is computed which is helpful in computing the response of a grating cell subunit. The activity of grating subunit **q** is computed using (6) which is either 0(non response) or 1(response). Here a threshold value (ρ=0.05) is used which is responsible for the response or non-response of grating subunit. In the next stage, the response of a grating cell is computed whose receptive field is centered on point (ξ, η) and which has a preferred orientation θ of the normal to the grating and periodicity λ (as taken above). The grating cell response is computed by weighted summation of the responses of the grating subunits. At the same time the model is made symmetrical for opposite directions by taking the sum of grating subunits with orientations θ and $\theta+\pi$ using equation (9). The parameter β is chosen as 6 for all images. Since the textural features of scene images show a wide range of wavelength and orientation, therefore a filter bank of eight grating cells can be used for a single image. The parameters of the eight grating cells are as follows:(λ=8.2,θ=22.5˚), (λ=8.2,θ=45˚), (λ=8.2,θ=67.5˚), (λ=8.2,θ=90˚), (λ=8.2,θ=112.5˚), (λ=8.2,θ=135˚), (λ=8.2,θ=157.5˚), (λ=8.2,θ=180˚) Pixel wise maximum superposition of all the filter outputs is performed and the resultant matrix obtained is the feature matrix. All the textural features of the input image are contained in the feature matrix .The matrix can be further used as input for the segmentation of the scene image using k-means clustering. We have been able to perform the segmentation of scene images (coast, mountain, open country, forest, building, highway) into two segments (k=2) and three segments (k=3).

In segmentation problem, the filter bank used respond differently to the different objects of scene.(for example strong response for one object, medium response for another and less or no response for the third object).Then the feature matrix is obtained. For segmentation, the feature matrix is passed through k-means clustering,(k=n).In our experiment n=2 and n=3 have been taken. As per this algorithm, n number of random mean clusters is taken randomly for n number of classes. Then Euclidean distance is calculated between every pixel of the image and the mean of the clusters. The pixel is allotted to that cluster where the Euclidean distance is minimum. This iteration is performed a number of times until we get n clusters whose means become constant. Then different grey values are assigned to the different clusters to get a segmented image.

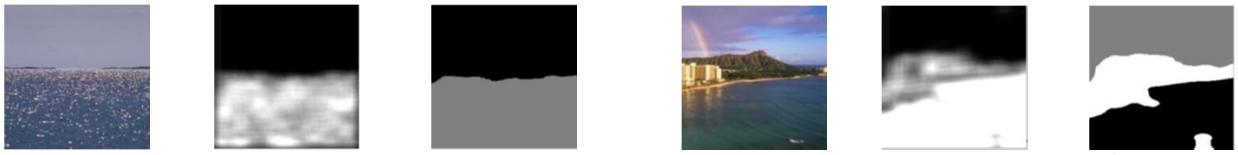

(a) (b) (c) (d) (e) (f)

Fig.2 Segmentation of images of coast using masksize=16, λ=8.2, θ=22.5˚,45˚,67.5˚,90˚,112.5˚,135˚,157.5˚,180˚ (a),(d) show the original images, (b),(e) correspond to their feature matrices and (c),(f) show their segmented images

(a) (b) (c) (d) (e) (f)

Fig.3 Segmentation of images of mountain using masksize=16, λ=8.2, θ=22.5˚,45˚,67.5˚,90˚,112.5˚,135˚,157.5˚,180˚, (a),(d) show the original images, (b), (e) correspond to their feature matrices and (c),(f) show their segmented images.

(a) (b) (c) (d) (e) (f)

Fig.4 Segmentation of images of open country using masksize=8, λ=8.2, θ=22.5˚,45˚,67.5˚,90˚,112.5˚,135˚,157.5˚,180˚, (a),(d) show the original images, (b), (e) correspond to their feature matrices and (c),(f) show their segmented images

(a). (b) (c) (d) (e) (f)

Fig.5 Segmentation of images of forest using masksize=16, λ=8.2, θ=22.5˚,45˚,67.5˚,90˚,112.5˚,135˚,157.5˚,180˚, (a),(d) show the original images, (b),(e) correspond to their feature matrices and (c),(f) show their segmented images

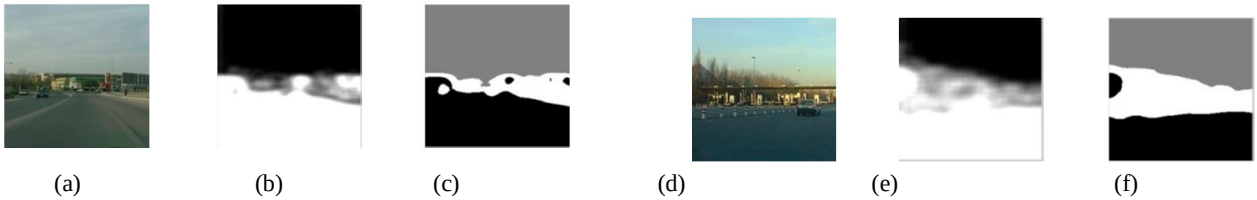

(a) (b) (c) (d) (e) (f)

Fig.6 Segmentation of images of highway using masksize=16, λ=8.2, θ=22.5˚,45˚,67.5˚,90˚,112.5˚,135˚,157.5˚,180˚, (a),(d) show the original images, (b),(e) correspond to their feature matrices and (c),(f) show their segmented images

Conclusion

We proposed a Grating cell texture operator that not only discriminates between textured and non-textured part of an image but also recognizes different kinds of texture. We have experimented on 100 scene images considering 20 images from each category. The textures respond differently to the grating cell based upon the parameters used. K-means algorithm has been used as the segmentation algorithm which gives good results with two or three region segmentation. Only inadequacy observed is that when there is a transistion from one segment to another at the boundary e.g. from white to black, there is a sharp transistion of pixel values. When summation is done at the boundary of those two segments, it results in average valued pixels at the boundary line, which don't belong to any of the meaningful segments. When k-means algorithm is applied, it appears like a new segmented area, which can be taken care of by reducing the area of summation but can't be completely eliminated. In future, in order to deal with complex scenes having more than three segments we intend to use more than one threshold value while computing grating cell response.

Acknowledgement

The authors express their hearty thanks to the department of Electronics and Telecommunication engineering, VSSUT, Burla,Odisha(India) for their support to this work.

References

[1] P. Kruizinga and N. Petkov, " Nonlinear Operator for Oriented Texture" IEEE transactions on image processing, vol. 8, no. 10, october 1999 ,139

[2] Junqing Chen, Thrasyvoulos N. Pappas,, Aleksandra Mojsilovi´c, and Bernice E. Rogowitz , "Adaptive Perceptual Color-Texture Image Segmentation," IEEE transactions on image processing, vol. 14, no. 10, october 2005 1

[3] Longsheng WEI, Dapeng LUO, and Xinmei WANG, "Active Contour Texture Image Segmentation Based on Anisotropic Diffusion" Journal of Computational Information Systems 10: 6 (2014) 2613–2620.

[4] Xiuwen Liu, and DeLiang Wang, "Image and Texture Segmentation Using Local Spectral Histograms", IEEE transactions on image processing, vol. 15, no. 10, october 2006

[5] S. Kothainachiar and Dr. R.S.D. Wahita Banu, "A Novel Image Segmentation based on a Combination of Colour and Texture Features," GVIP Journal, Volume 7, Issue 2, August, 2007

[6] Wenbing Tao, Hai Jin, Senior Member, IEEE, and Yimin Zhang, Senior Member, IEEE "Color Image Segmentation Based on Mean Shift and Normalized Cuts" IEEE transactions on systems, man, and cybernetics—part b: cybernetics, vol. 37, no. 5, october 2007

[7] Ajay K. Mishra, Yiannis Aloimonos, Loong-Fah Cheong, and Ashraf A. Kassim, Member, IEEE "Active Visual Segmentation" IEEE transactions on pattern analysis and machine intelligence, vol. 34, no. 4, april 2012

[8] Computational Visual Cognition Laboratory,Auda Olivia, Ph.D, (http://cvcl.mit.edu/database.htm)

[9] R. Von der Heydt , E. Peterhans and M.R Dursteler, "Grating cells in monkey visual cortex: coding texture?" in channels in the visual Nervous system: Neurophysiology, Psychophysics and Models, B. Blum, Ed. London, U.K : Freund, 1991, pp 53-73

[10] A. Bosch , X. Munoz, J. Freixenet, *Segmentation and description of natural outdoor scenes Image and Vision Computing* (2006)

[11] Xiaoru Wang, Junping Du, Jie Liu, "A Semantic based segmentation algorithm for scene images" Proceedings of IEEE CCIS2011, 2011

[12] Chang Cheng, Andreas Koschan, Chung Hao Chen, David L. Page, Mongi A Abidi, "Outdoor scene segmentation based on Background recognition and perceptual organization", IEEE Transactions on image processing, vol 21, No 3, March 2012